




Article

Machine Learning-Based Model Prediction of an Adsorption Desalination System and Investigation of the Impact of Parameters on the System's Outputs

Taleb Zarei ^{1,*}, Masoud Chatavi ², Masoud Nazari ¹, Amirhossein Amirfakhraei ³, Mohsen Salimi ^{4,*} and Majid Amidpour ³

¹ Department of Mechanical Engineering, University of Hormozgan, Bandar Abbas 7916193145, Iran; masoud.nazari1995@gmail.com

² Mechatronics Engineering Group, Amirkabir University of Technology, Tehran 1591634311, Iran; m_ch@aut.ac.ir

³ Faculty of Mechanical Engineering, Department of Energy System Engineering, K.N. Toosi University of Technology, Tehran 1996715433, Iran; a.amirfakhraei@gmail.com (A.A.); amidpour@kntu.ac.ir (M.A.)

⁴ Renewable Energy Research Department, Niroo Research Institute (NRI), Tehran 1468613113, Iran

* Correspondence: talebzarei@hormozgan.ac.ir (T.Z.); msalimi@nri.ac.ir (M.S.)

Abstract: Adsorption desalination (AD) has emerged as a novel technique for desalination, which works cyclically and via switching, and various variables have an effect on its performance. This study uses machine learning procedures to present a model predictive approach for adsorption desalination systems. The adsorption desalination system will be modeled through the utilization of multilayer perceptron (MLP) and radial-based function (RBF) neural network approaches. The purpose of this research is to provide valuable insights into optimizing system efficiency and expanding the applicability of adsorption desalination technologies by investigating the strengths and limitations of each model. Hence, the Specific Daily Water Production (SDWP), coefficient of performance (COP), and specific cooling power (SCP) are determined. There are 55 instances in the dataset, each with five input variables: temperatures of the evaporator and condenser, adsorption beds, and inlet hot saltwater. Additionally, three output variables are recorded: COP, SCP, and SDWP. The results of this investigation show that the MLP is more effective for simulating the AD system, and the Roots of Mean Square Error of COP, SCP, and SDWP are 0.002, 0.5921, and 0.0465, respectively. Then, the impact of input factors on output parameters was examined. The results show that the inlet hot saltwater temperature parameter affected the output parameters the most. Subsequently, the COP parameter is mainly affected by the adsorption beds, evaporator, and condenser temperature. The SCP parameter is primarily influenced by the inlet hot saltwater temperature, condenser temperature, temperatures of the two adsorption beds, and evaporator temperature.

Keywords: desalination; adsorption desalination system; artificial neural network; model predictive



Citation: Zarei, T.; Chatavi, M.; Nazari, M.; Amirfakhraei, A.; Salimi, M.; Amidpour, M. Machine Learning-Based Model Prediction of an Adsorption Desalination System and Investigation of the Impact of Parameters on the System's Outputs. *Water* **2024**, *16*, 3700. <https://doi.org/10.3390/w16243700>

Received: 26 October 2024

Revised: 15 December 2024

Accepted: 17 December 2024

Published: 22 December 2024



Copyright: © 2024 by the authors. Licensee MDPI, Basel, Switzerland. This article is an open access article distributed under the terms and conditions of the Creative Commons Attribution (CC BY) license (<https://creativecommons.org/licenses/by/4.0/>).

1. Introduction

Water is regarded as the fundamental substance necessary for sustaining life. Water covers about 71% of the surface of the earth. Approximately 97% of the earth's seawater is characterized by its salinity, while the remaining 2% comprises frozen water in the nature of glaciers and ice. Therefore, the remaining global water resources are a valuable and indispensable asset crucial for our continued existence [1]. The issue of inadequate access to clean water for a livelihood is a significant global challenge that necessitates immediate consideration. The global demand for freshwater is increasingly emerging as a significant concern. Access to drinkable water is critical for establishing human habitats in dry regions where water scarcity is prevalent [2]. Water consumption can be checked in two parts: The first part is the consumption of water for drinking and domestic use, which uses the

water of some lakes and rivers and is finally purified and used. The second part of water consumption is in cooling and water needed by industries, which mainly use salty sea and ocean waters, which must first be desalinated with the help of industrial desalination methods. Various techniques have been developed and implemented for the desalination of saltwater, including multi-effect distillation (MED), multi-stage flash (MSF), and reverse osmosis (RO), which have entered the commercial market. One emerging desalination technique is adsorption desalination (AD), which exhibits significantly reduced energy usage compared to conventional desalination technologies commonly employed in the industry. The approach exhibits several advantages that facilitate the industrialization of this technology because it does not necessitate a significant amount of energy, uses wasteful and renewable energy sources, produces little pollution, and has low maintenance and repair costs. A schematic of desalination methods is depicted in the Figure 1, which shows that the adsorption desalination method is a subset of the thermal method.

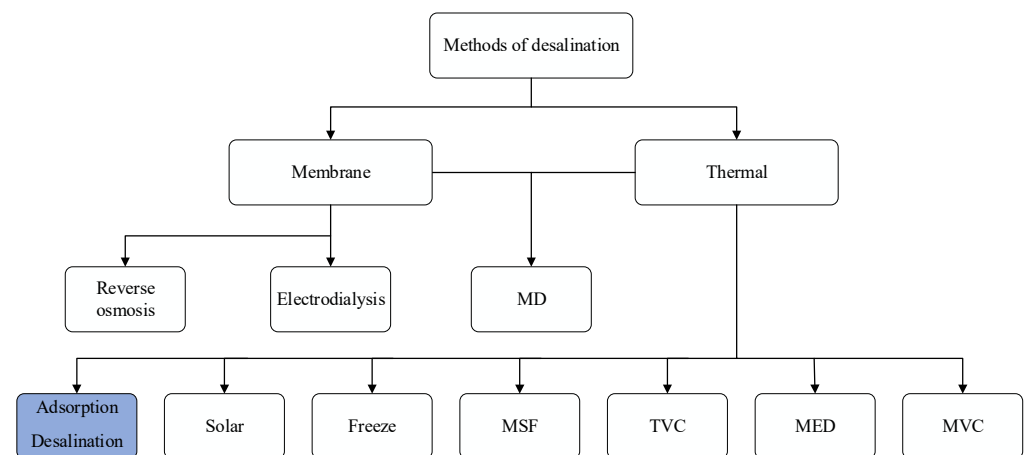


Figure 1. Different methods for the desalination of seawater and saltwater.

In this study, the performance of an adsorption desalination system, which has a cyclic operation with a complex control system, was modeled via a machine learning procedure. This research used two different machine learning models, including the multilayer perceptron (MLP) and radial-based function (RBF) neural network approaches. These models are used to predict critical parameters, such as COP, SCP, and SDWP, using input data that include evaporator and condenser temperatures, adsorption beds, and hot water entering the system. This study makes a significant contribution by conducting a comprehensive comparative analysis of these machine learning models, revealing their efficacy in predicting key performance indicators of the adsorption desalination system. The purpose of this research is to provide valuable insights into optimizing system efficiency and expanding the applicability of adsorption desalination technologies by investigating the strengths and limitations of each model. As a result, this comparative study could add a new perspective to ongoing efforts to address water scarcity through sustainable and energy-efficient means. Meanwhile, due to the limited amount of data required for machine learning models in such scenarios, selecting an appropriate model capable of effectively training and predicting data is crucial. Considering the complexity of the adsorption desalination system, the effect of various parameters on the performance of the system in terms of water production and energy consumption is another goal of this research.

This technique aims to develop a more streamlined model to address the intricate challenges associated with multi-domain molecular and numerical simulation. The subsequent analysis presents an outline of the organizational framework. Section 2 provides an introduction to the background of the research. The adsorption desalination system is briefly presented in Section 3. Based on objectives defined to predict the model, the artificial neural network, and its algorithms, the MLP and RBF are discussed in Section 4. In Section 5, these approaches are simulated and compared with the analytical approach.

Then, in Section 6, based on predefined criteria, the performance of the predicted model is evaluated, and the efficacy of input parameters on each output is investigated.

2. Background

Given the substantial investment and high energy requirements associated with desalination systems, researchers have explored approaches to mitigate energy usage [3–8]. Here, the history of the adsorption desalination system (ADS), a subset of thermal desalination, was investigated. Before 2004, extensive studies had been conducted on adsorption chillers. However, the potential integration of these chillers with desalination systems has not been previously explored. The first studies focusing on the production of freshwater using adsorption systems were conducted by Zejli et al. (2004), who simulated adsorption desalination systems with the help of plan transfer from adsorption chillers, with the difference that in chillers, adsorption is a closed thermodynamic cycle. However, in desalinated water, the thermodynamic cycle is open. In this system, the adsorbent material used is zeolite, and the amount of energy consumption and produced water is studied [9].

In a study conducted in 2007, Wang et al. studied the impact of a mass and energy recovery strategy on the efficiency of an AD system. Through two simultaneous experimental investigations, one with the implementation of the recovery strategy and the other without, the researchers observed a significant enhancement in process performance. Specifically, the recovery strategy resulted in a 42.7% improvement in overall system performance and a 15.7% increase in water production [10]. In a study conducted in 2016, Mitra et al. employed a simulation of a two-stage system consisting of adsorbent beds. Their research aimed to investigate this system's impact on the thermodynamic cycle's continuity and the quantity of water generated. Their findings revealed a favorable influence in both aspects [11]. Research by Ali et al. in 2016 sought to examine the function of two distinct adsorbents inside a two-stage desalination cycle. In this manner, the researchers evaluated the advantages and superiority of various materials concerning the requirement for increased production of water or cooling [12].

Adsorption desalination systems (ADSs) have captured much attention due to the utility of waste heat as well as renewable energy resources. Amir Fakhraei et al. [13] proposed various scenarios for mass and heat recovery inside the ADS. Compared to the conventional systems, without a heat and mass recovery mode, improvements of about 200 and 51 percent, regarding the amount of water produced and the performance ratio, were observed, respectively.

Also, some research has been conducted in the domain of saltwater desalination utilizing machine learning. In 2019, Zarei et al. employed neural networks for modeling and optimizing a seawater greenhouse that was employed from HDH desalination. They further examined the impact of changes in the dimensions of the greenhouse across both the complete cycle and half cycle on the system's output parameters. The outcome entailed a decrease in the temperature of the generated water, an increase in the amount of generated water, and an improvement in the system's efficiency [14,15].

Essa et al. [16] modeled a type of solar desalination with the help of ANN and a support vector machine network (SVM) and, in that model, predicted the quantity of water generated by the system. In 2018, Cabrera et al. modeled the seawater reverse osmosis (SWRO) desalination system using three methods: artificial ANN, SVM, and random forest. They then evaluated the performance of this system [17]. A solar desalination system, featuring a single-slope solar still, was studied in [18]. For the mentioned design, Al_2O_3 nanofluid is employed, and the optimal conditions for maximizing both efficiency and cost-effectiveness are determined through the application of a reinforcement learning technique known as a deep Q-value neural network (DQN). The efficacy of an RO desalination plant based on permeate conductivity was investigated using deep learning long short-term memory (LSTM) in conjunction with an optimized crow search algorithm (CSA), and the results proved that ANN could optimize energy consumption [19]. The integration of advanced computational techniques and machine learning (ML) has been employed to

enhance the design of materials for desalination purposes. Global optimization algorithms have been utilized to improve the desalination efficiency of membranes. A promising candidate for desalination membranes, composed of $\text{Ti}_3\text{C}_2\text{O}_2$, has been identified, featuring a specific charge at the mouth of its nanopores. Furthermore, a physical–chemical analysis investigated how the charge at the MXene nanopore mouth influences the overall desalination performance [20].

In 2021, Faegh et al. [21], for the first time, investigated a humidification–dehumidification desalination system with the help of neural networks; in this research, they designed three models of MLP, RBF, and the adaptive neuro-fuzzy inference system (ANFIS) with 180 test samples. The gain output ratio (GOR), heat transfer rates of the evaporator, and evaporative condenser were considered outputs. Out of the several models that were built, it was found that the MLP exhibited the most accurate predictions for the target parameters. Shahouni et al. [22] summarized the utilization of artificial intelligence in forecasting the behavior of membranes, highlighting their advantages, limitations, and prospective advancements in the application of artificial intelligence (AI) for water desalination processes.

As seen, the use of an artificial neural network (ANN) has been used in various desalination systems. In recent years, this ability has been used to predict the behavior of absorption desalination. For the first time, in 2021, Alhumade et al. [23] modelled the output performance of ADS in terms of switching and cycle time using artificial intelligence. The outcomes confirmed the superiority of ANFIS modeling of the output performance of the adsorption desalination system compared with regression. Zayed et al. [24] investigated the performance of a solar adsorption desalination system (SADS). The system produced $6.30 \text{ m}^3/\text{ton-day}$ with a specific cooling power of 153 W/kg . An ANFIS was employed to model the system, and a manta ray foraging optimizer (MRFO) was used to explore the optimal ANFIS structure. This ANFIS-MRFO approach demonstrated exceptional accuracy in predicting the performance of the SADS.

Numerous theoretical and experimental studies with different numerical solutions have been proposed in the literature to develop models and analyze parameters in various systems. Due to the complexity of the dynamical and molecular modeling of desalination systems, numerical solution approaches are costly, time-consuming, and susceptible to calculation errors. Machine learning approaches are characterized by their reliance on data and ability to operate independently of the underlying system dynamics, even when knowledge is insufficient. These abilities enable the prediction of accurate models and the analysis of parameter efficiency on outputs.

3. Adsorption Desalination System

Adsorptive desalination (AD) is a newly emerging method that uses low-temperature heat sources and waste heat energy to desalinate saline waters, usually including one or more distillation steps to produce steam. Since the AD system is mainly started with low energy, this system can be used with low-temperature renewable energy sources, especially solar energy and industrial waste heat. In adsorption systems, it is possible to place a cooling cycle; therefore, compared to alternative desalination technologies, it may be argued that this particular approach exhibits a comparatively higher level of efficiency and environmental friendliness [11]. Solid adsorbent materials, such as silica gel and zeolite, absorb and store steam and maintain steam's partial pressure to accelerate evaporation. Hot water is almost always used in this process, and sometimes electricity is needed to run the pumps.

Furthermore, the utilization of heat within a temperature range of $55\text{--}85 \text{ }^\circ\text{C}$ proves to be advantageous in this process. This is particularly notable as it allows for the utilization of heat derived from renewable energy sources or waste heat generated by industrial activities. A typical AD system is depicted in Figure 2. The main components of adsorption systems encompass sorption elements (SEs) in the form of adsorption beds and condensers, along with additional components, such as condensers, evaporators, hot water tanks, cooling tow-

ers, and auxiliary elements, including pumps, feeding tanks, collection tanks, and saltwater tanks. SE intermittently occurs between the adsorption and excretion phases [5,9,11,25,26].

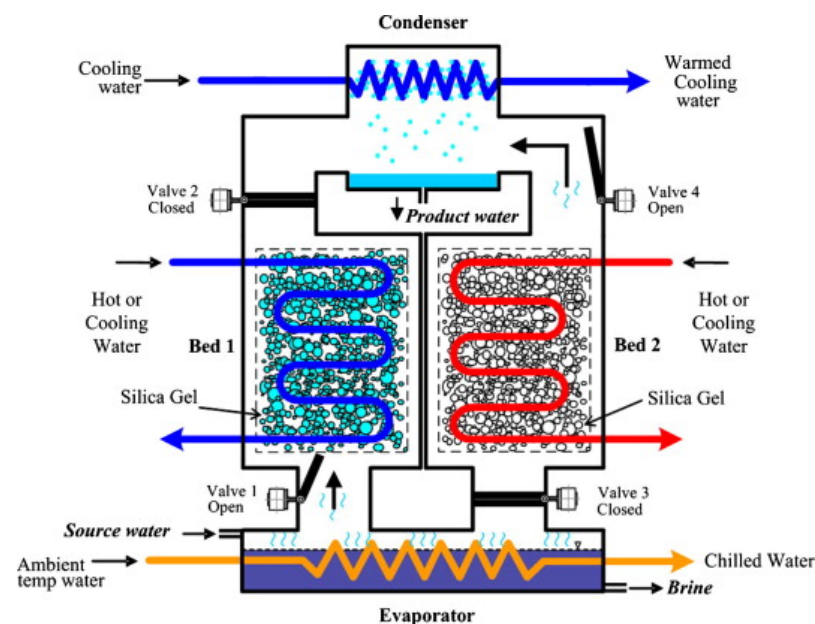


Figure 2. Schematic of two-bed ADS. Adapted with permission from [27] 2012, Wu, Jun, W.

A prototypical two-bed adsorption–desorption cycle can be delineated as follows: The seawater is conveyed from the feeding tank to the evaporator, which undergoes heating. Subsequently, the adsorbent in bed one continually absorbs the resulting steam until it reaches saturation. During this time, the cooling water is circulated throughout the bed in order to remove the heat that has been adsorbed. During the subsequent phase, bed one undergoes a transition into rejection mode, wherein the circulation of hot water inside it raises the adsorbent material temperature, finally releasing steam. Then, the regenerated steam is sent towards the condenser, where it undergoes condensation before being transferred to the flow collection tank [28]. In specialized adsorption systems, internal heat recovery is utilized to recover energy during the transition phase when the adsorption bed and disposal bed are exchanged. During the exchange period, there exists a significant disparity in temperature between the adsorbent bed, which remains at elevated levels, and the adsorbent bed, which experiences a notable decrease in temperature. Direct displacement results in a notable rise in the temperature of the cooling water outlet while concurrently causing a fall in the hot water outlet. In the given situation, an internal heat recovery cycle is employed to enable the transfer of surplus heat from the desorption bed to the adsorption bed, hence allowing for its efficient utilization. Both numerical and experimental investigations have provided evidence that the integration of this heat recovery approach significantly improves the energy efficiency of the anaerobic digestion system [3].

4. Artificial Neural Networks

Artificial neural networks (ANNs) are highly effective at approximating nonlinear multi-input and multi-output functions with the desired accuracy using supervised input–output pair data. Moreover, ANNs work independently of the system structure, resulting in stable implementation, regardless of unforeseen alterations. Artificial neural networks are widely recognized as a prominent machine learning methodology utilized for data processing via successive layers of analysis. The nomenclature of artificial neural networks is derived from their resemblance to the organization and operation of the human brain. The human brain comprises a network of interconnected neurons, each possessing dendrites that serve as receptors for receiving inputs. The neuron receives input signals, which it

subsequently transforms into electrical signals. These electrical signals are then transmitted through the axon and propagated to other neurons via the axon terminals. The artificial neuron serves as the essential component within an ANN. It is a mathematical construct designed to emulate the functionality of a biological neuron.

Hence, the input data are transmitted to the artificial neuron, and after mathematical processing, it can result in an output. Before the neuron receives the input data, weights are assigned to the input parameters to replicate the stochastic characteristics of the biological neuron. The model prediction process using ANN is introduced in Figure 3.

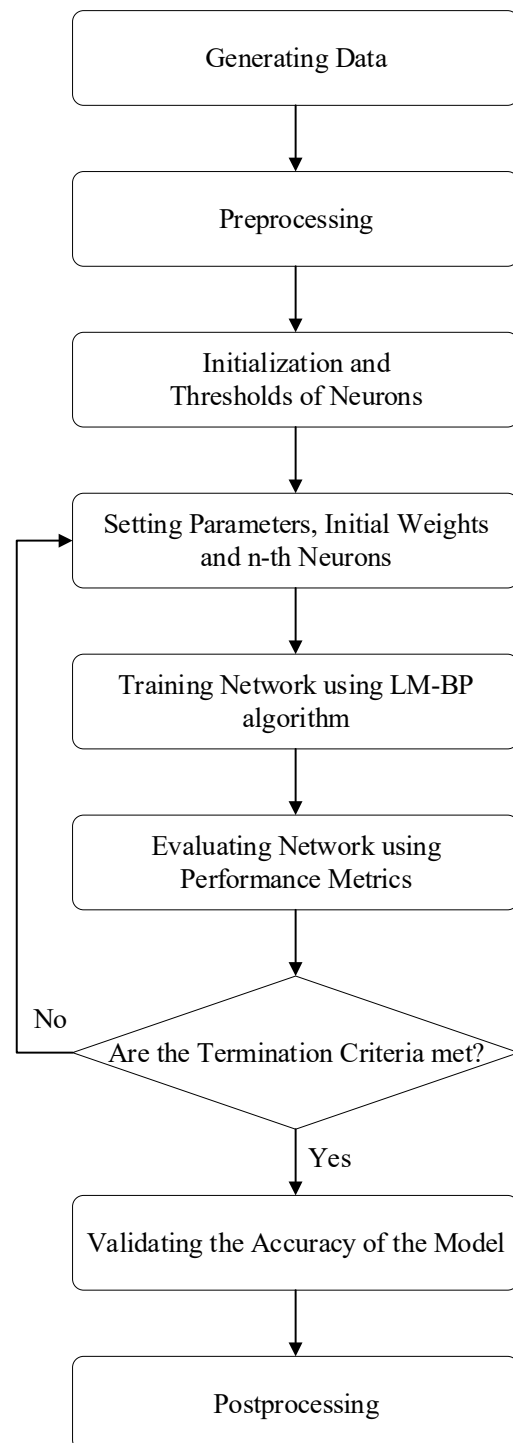


Figure 3. The process of training and evaluating ANN.

4.1. Multilayer Perceptron Neural Network

The multilayer perceptron (MLP) is the most commonly employed artificial neural network (ANN) for addressing linear and nonlinear problems. MLP is a computational model typically consisting of three distinct phases: an input layer, a hidden layer, and an output layer. Each layer comprises a varying number of neurons (Figure 4). The hidden layer(s) is responsible for processing data received from the input layer and transmitting these signals to the output layer. Nonlinear and continuously differentiable functions such as sigmoid, hyperbolic tangent, or any other suitable function can be utilized in the hidden layer. In order to optimize the effectiveness of training, it is standard to choose the linear function for the output layer. An essential concern in perceptron networks is determining the optimal number of hidden layers and neurons, typically achieved by iterative experimentation [29].

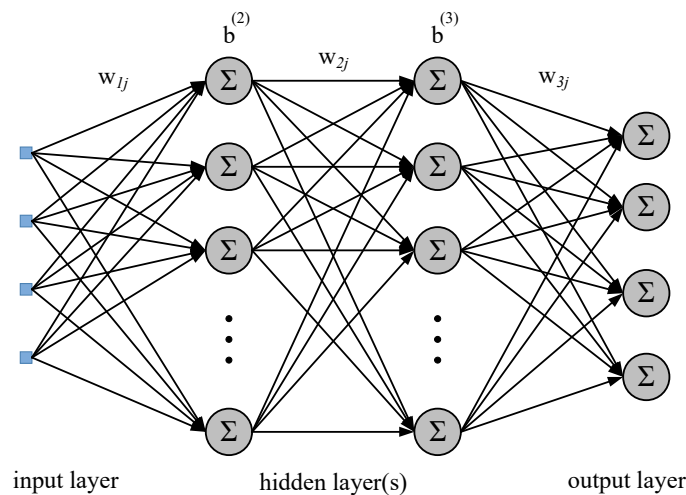


Figure 4. Configuration of MLP neural network.

4.2. Radial Basis Function Neural Network

Radial basis function (RBF) neural networks were introduced in 1988. These networks have garnered considerable attention due to their strong generalization capabilities and straightforward network construction, which minimizes unnecessary and lengthy computations compared to MLP networks. Previous studies on universal approximation theorems in the context of RBF have demonstrated that it is possible to estimate any nonlinear function over a compact set with high accuracy [30].

The configuration of layers of an RBF neural network is identical to that of an MLP. The activation of neurons in the hidden layer is achieved by employing a radial basis function. The hidden layer comprises a set of computational units known as hidden nodes. Figure 5 illustrates the structure of a conventional three-layer radial basis function (RBF) neural network [30].

In the RBF neural network, $x = [x_i]^T$ is the input vector. Assuming there are m -th neural nets, and the radial basis function vector in the hidden layer of RBF is $h = [h_j]^T$, h_j is a Gaussian function value for neural net j in the hidden layer, and

$$h_j = \exp\left(-\frac{\|x - c_{ij}\|^2}{2b_j^2}\right) \tag{1}$$

where $c = [c_{ij}] = \begin{bmatrix} c_{11} & \cdots & c_{1m} \\ \vdots & \ddots & \vdots \\ c_{n1} & \cdots & c_{nm} \end{bmatrix}$ represents the coordinate value of the center point of the Gaussian function of neural net j for the i th input, $i = 1, 2, \dots, n, j = 1, 2, \dots, m$.

The vector $\mathbf{b} = [b_1 \dots b_m]^T$ represents the width value of the Gaussian function for neural net j .

The weight value of RBF is

$$\mathbf{W} = [W_1 \dots W_m]^T. \quad (2)$$

The output of the RBF neural network is

$$y(t) = \mathbf{W}^T \mathbf{h} = W_1 h_1 + W_2 h_2 + \dots + W_m h_m \quad (3)$$

The Levenberg–Marquardt backpropagation (LM-BP) algorithm is arguably one of the most popular learning algorithms. LM optimization is often the fastest BP algorithm and is highly recommended as a first-choice supervised algorithm. During this procedure, the weight and bias variables are modified based on the Levenberg–Marquardt (LM) method, while the backpropagation (BP) algorithm is employed to compute the Jacobian matrix of the performance function concerning the weight and bias variables [30].

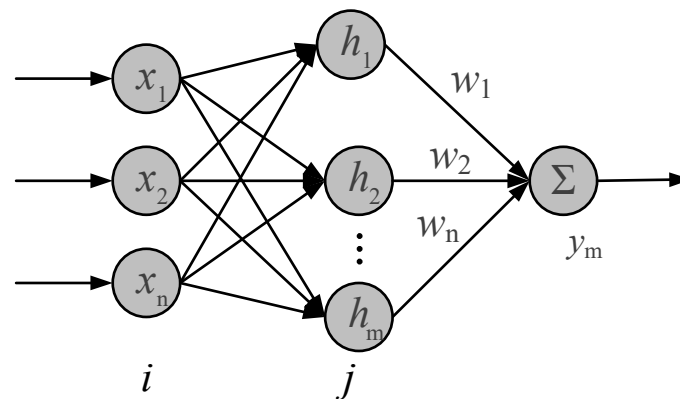


Figure 5. Configuration of RBF neural network.

5. Simulation

In this study, the present ADS without mass and heat recovery model is based on Alsaman et al.'s [5] experimental work. Table 1 shows the operating conditions of this AD cycle [5].

Table 1. Operating conditions of conventional AD cycle [5].

Parameters	Value	Unit
Bed heat transfer coefficient	600	W/K
Evaporator heat transfer coefficient	350	W/K
Condenser heat transfer coefficient	500	W/K
Weight of bed hex fin (Al)	0.72	Kg
Weight of bed hex tube (Cu)	2.97	Kg
Weight of evaporator hex tube (Cu)	1.3	Kg
Silica gel Weight	6.75	Kg
Weight of condenser hex tube (Cu)	1.535	Kg
Cover weight of bed (Iron)	15	Kg
Evaporator Liquid seawater	3	Kg
Silica gel particle radius	0.00175	m
Temperature of cold source	30	(°C)
Temperature of chilled water	30	(°C)
Temperature of hot source	75–95	(°C)
Flow rate of cold water	0.3	Kg/s
Flow rate of chilled water	0.025	Kg/s
Flow rate of hot water	0.2	Kg/s
Cycle time	650	s

This research focuses on analyzing an adsorption desalination system, aiming to develop a predictive model and evaluate the influence of different parameters on the system's outputs. The system incorporates five input variables, including the temperature parameters of the AD equipment. These variables consist of the inlet hot water temperature, evaporator temperature, condenser temperature, and the temperatures of adsorption beds one and two. The output variables include the COP, SCP, and SDWP.

Since the ANN is data-driven, 55 data are extracted from Al-Saman et al.'s article [5]. The dataset is partitioned into three subsets, namely training, validation, and test data, to evaluate the model's efficacy and avoid the issues of underfitting and overfitting. Moreover, due to the varying ranges of variables, it is recommended to employ data normalization techniques.

This study utilizes MLP and RBF neural networks to address the specified research objectives. In order to evaluate the efficacy and accuracy of the prediction model, a range of statistical measures are employed, such as the maximum absolute error, Mean Absolute Error (MAE), the Roots of Mean Square Error (RMSE), the standard deviation of the error, and linear regression.

The examined AD system comprises five inputs and three outputs. Therefore, an ANN is taken into consideration for every output. This structure has several benefits, namely a reduced learning period and enhanced precision, as ANN weights are specifically designed for a singular objective. The configuration of MLP consists of a layer with five neurons with a sigmoid tangent activation function. The available data are divided so that 85% were used for training and validating and 15% for testing the model. The configuration of RBF consists of a layer with 55 neurons with a spread of 2. The available data are divided so that 80% are used for training and validating and 20% for evaluating the model. Levenberg–Marquardt backpropagation (LM-BP) was used in this method due to its better efficiency and quick response.

The Levenberg–Marquardt backpropagation (LM-BP) algorithm is arguably one of the most popular learning algorithms. LM optimization is often the fastest BP algorithm and is highly recommended as a first-choice supervised algorithm. In this process, the weight and bias variables are adjusted according to the LM method, and the BP algorithm is used to calculate the Jacobian matrix of the performance function concerning the weight and bias variables.

The BP algorithm consists of two phases: The feedforward pass involves the computation of the ANN's output value(s) for each training pattern. On the other hand, backward propagation refers to propagating an erroneous signal from the output layer towards the input layer. The adjustment of weights is performed based on the backpropagated error signal. The LM optimization method combines the advantages of Newton's approach, which exhibits quick convergence towards a minimum but may potentially diverge, and Gradient descent, which ensures convergence by appropriately selecting the step-size parameter but converges gradually. Consider optimizing a second-order function $F(x)$, and let g be its gradient vector and H be its Hessian. According to the LM method, the optimum adjustment Δx applied to the parameter vector x is defined by [31,32]

$$F(x) = x_{k+1} - x_k = [H + \mu I]^{-1}g \quad (4)$$

where I is the identity matrix of the same dimensions as H , and μ is a regularizing or loading parameter that forces the sum matrix to be positive definite and safely well-conditioned throughout the computation.

The regularization parameter determines which method of LM is more effective; if the scalar μ is zero, Newton's method employs an approximate Hessian matrix. When μ is large, gradient descent with a small step size occurs. Consequently, this study considers a range of [0.001, 1000] for the regularization parameter. The learning rate of the ANN calculates the number of weights developed for each training iteration. In general, it can be observed that when the learning rate is set at a low value, the algorithm tends to require a significant amount of time to converge. Conversely, the method's stability becomes

compromised if the learning rate is set considerably high. Therefore, a learning rate in the [0.01, 0.8] range is recommended to ensure the system’s stability.

6. Results of the Predicted Models with Neural Networks

The preceding phase involved examining the adsorption desalination system with two beds, utilizing the MATLAB 2018b software’s artificial neural networks (ANNs). This study encompasses the design of six distinct models, with subsequent presentation of the outcomes and corresponding diagrams for each model. In the context of neural networks, determining the optimal number of neurons and hidden layers is typically achieved through an iterative process of experimentation and refinement. In order to assess the effectiveness of neural networks, multiple metrics are employed to analyze the network and its performance. Subsequently, the optimal model is chosen based on the evaluation criteria and the resultant graphical representations.

6.1. Results of the Predicted Models for the System Outputs

6.1.1. Results of the Predicted Models for the COP Parameter

In order to evaluate the predicted models, the test data are used. Figures 6 and 7 present the output results for the COP output parameter obtained from the MLP and RBF neural network models, respectively:

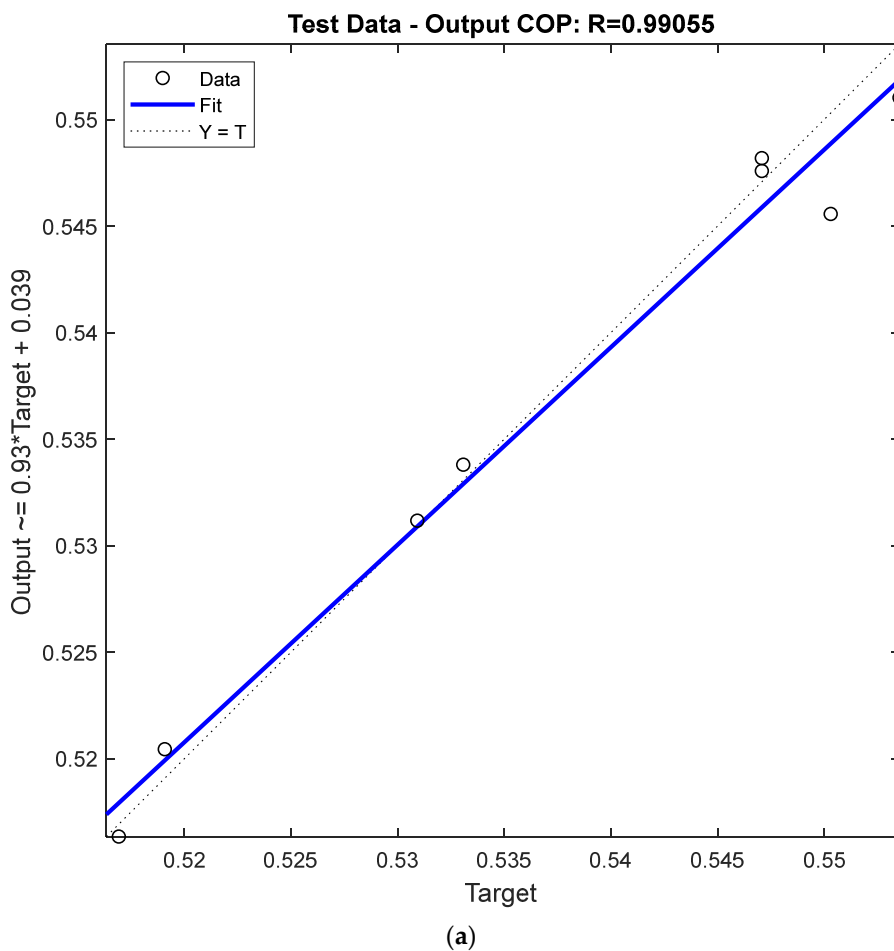


Figure 6. Cont.

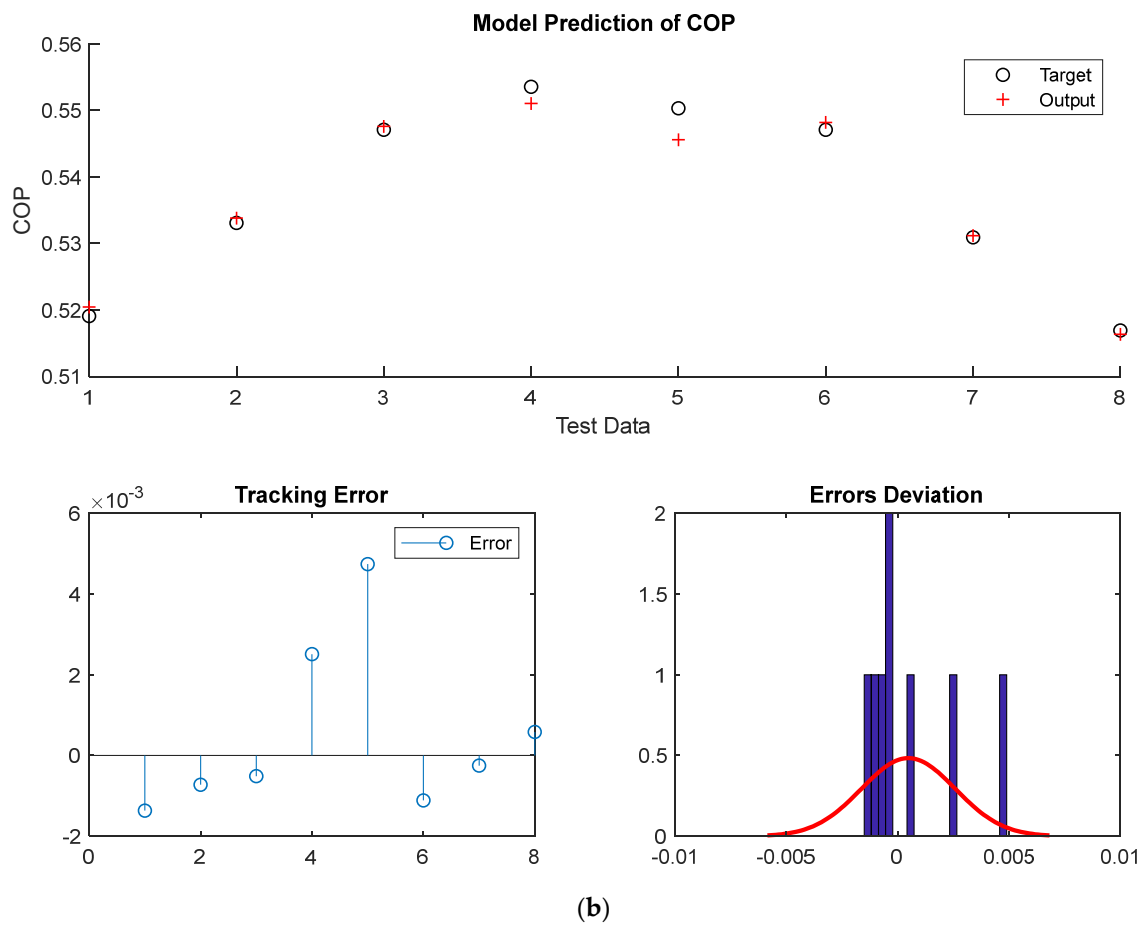


Figure 6. (a) Regression diagram of test data of MLP neural network for COP parameter. (b) The test data error for the MLP model in predicting the COP parameter.

Considering that a better model is designed whose regression (R) is closer to one and the value of its error indicators is closer to zero, from examining the regression diagram of both methods, it is concluded that the performance of the MLP is better and has a regression value of $R = 0.9905$ and RMSE value of 0.00203. Based on the analysis of error graphs and error histograms, it was observed that the radius-based functional neural network (RBF) had limited predictive capability for both the test and experimental data. Furthermore, by examining the RMSE indices, MAE, and other parameters in Figure 8, it was found that the MLP neural network exhibited superior performance for predicting the COP parameter over the RBF neural network.

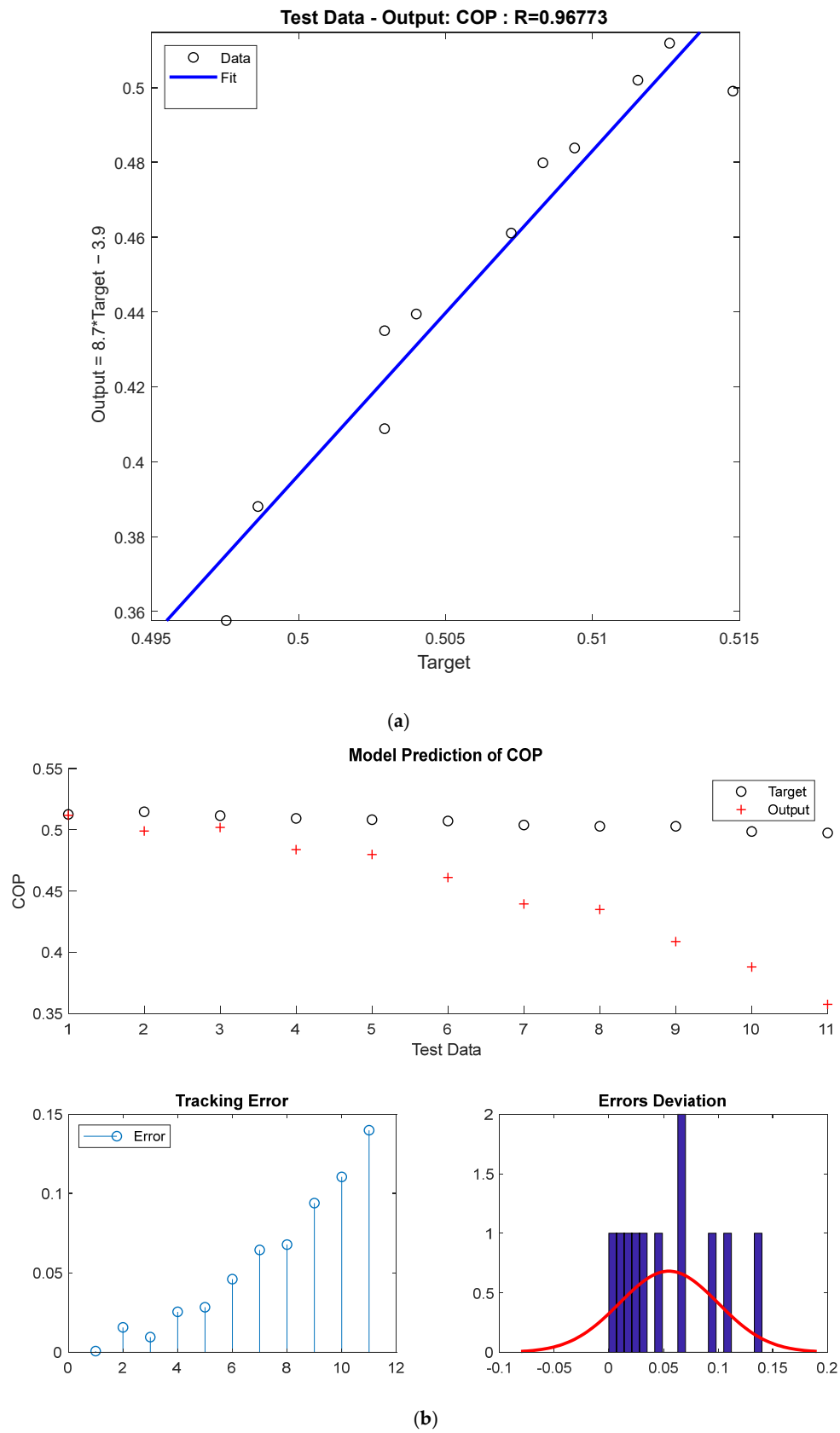


Figure 7. (a) Regression diagram of test data of RBF neural network for COP parameter. (b) The test data error for the RBF model in predicting the COP parameter.

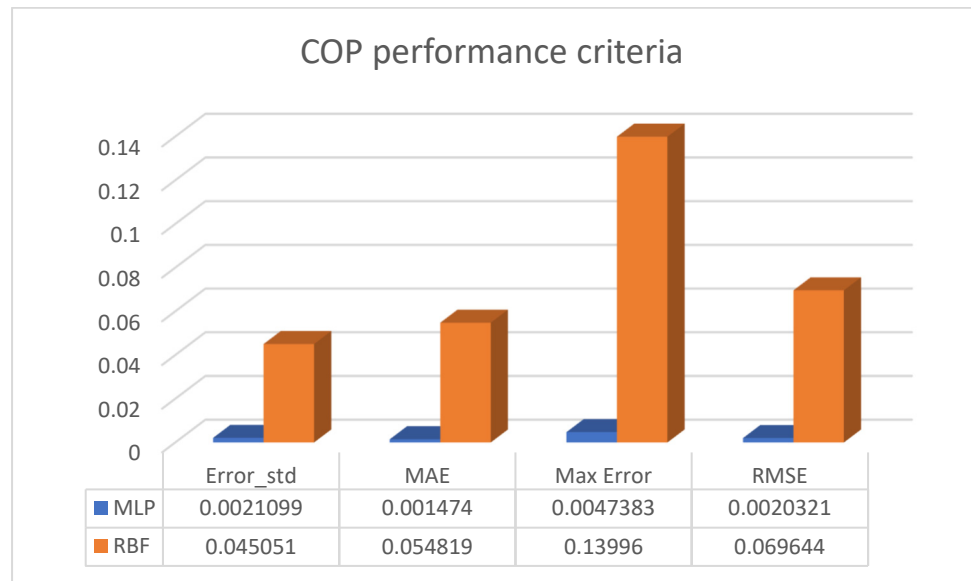


Figure 8. Evaluation metrics of MLP and RBF neural networks for COP parameter.

6.1.2. Results of the Predicted Models for the SCP Parameter

In order to evaluate the predicted models, the test data are used. Figures 9 and 10 present the output results for the SCP output parameter obtained from the MLP and RBF neural network models, respectively:

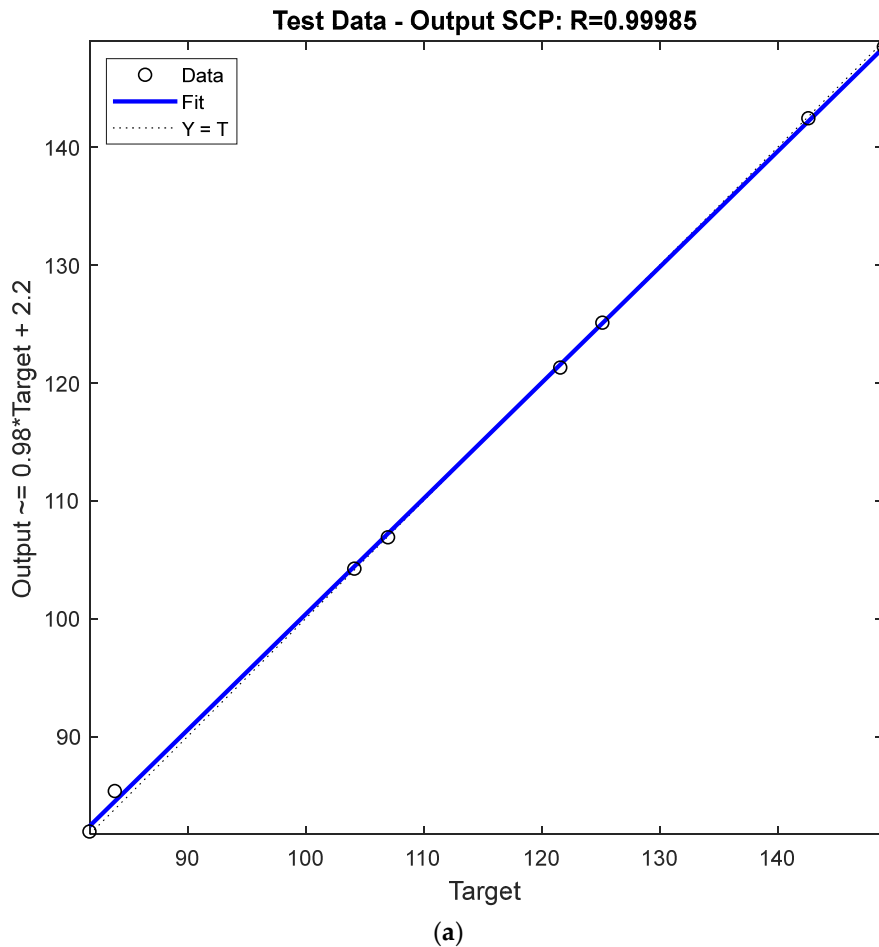


Figure 9. Cont.

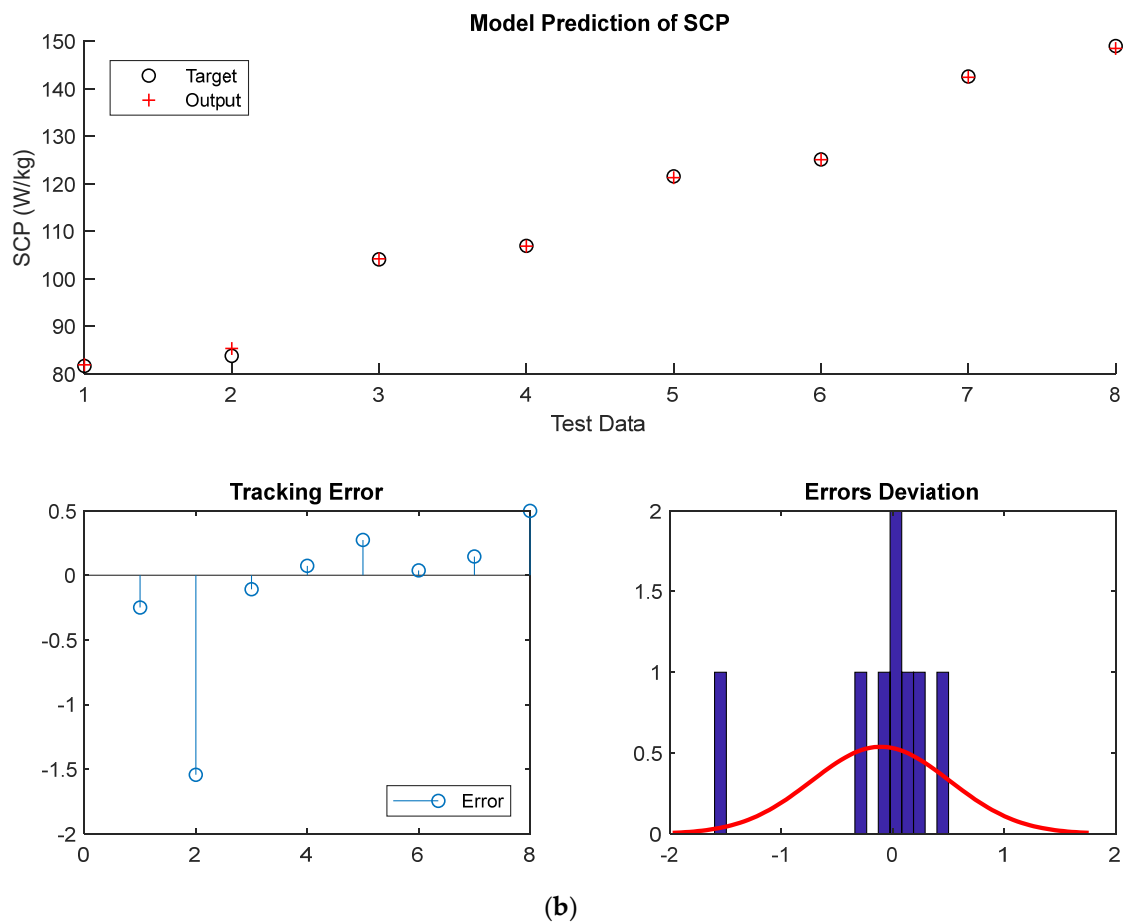


Figure 9. (a) Regression diagram of test data of MLP neural network for SCP parameter. (b) The test data error for the MLP model in predicting the SCP parameter.

Considering that a better model is designed whose regression (R) is closer to one and the value of its error indicators is closer to zero, from examining the regression diagram of both methods, it is concluded that the performance of the MLP is better and has a regression value of $R = 0.9998$ and RMSE value of 0.5921. Based on the analysis of error graphs and error histograms, it was observed that the radius-based functional neural network (RBF) had limited predictive capability for both the test and experimental data. Furthermore, by examining the RMSE indices, MAE, and other parameters in Figure 11, it was found that the MLP neural network had a better performance for predicting the SCP parameter than the RBF neural network.

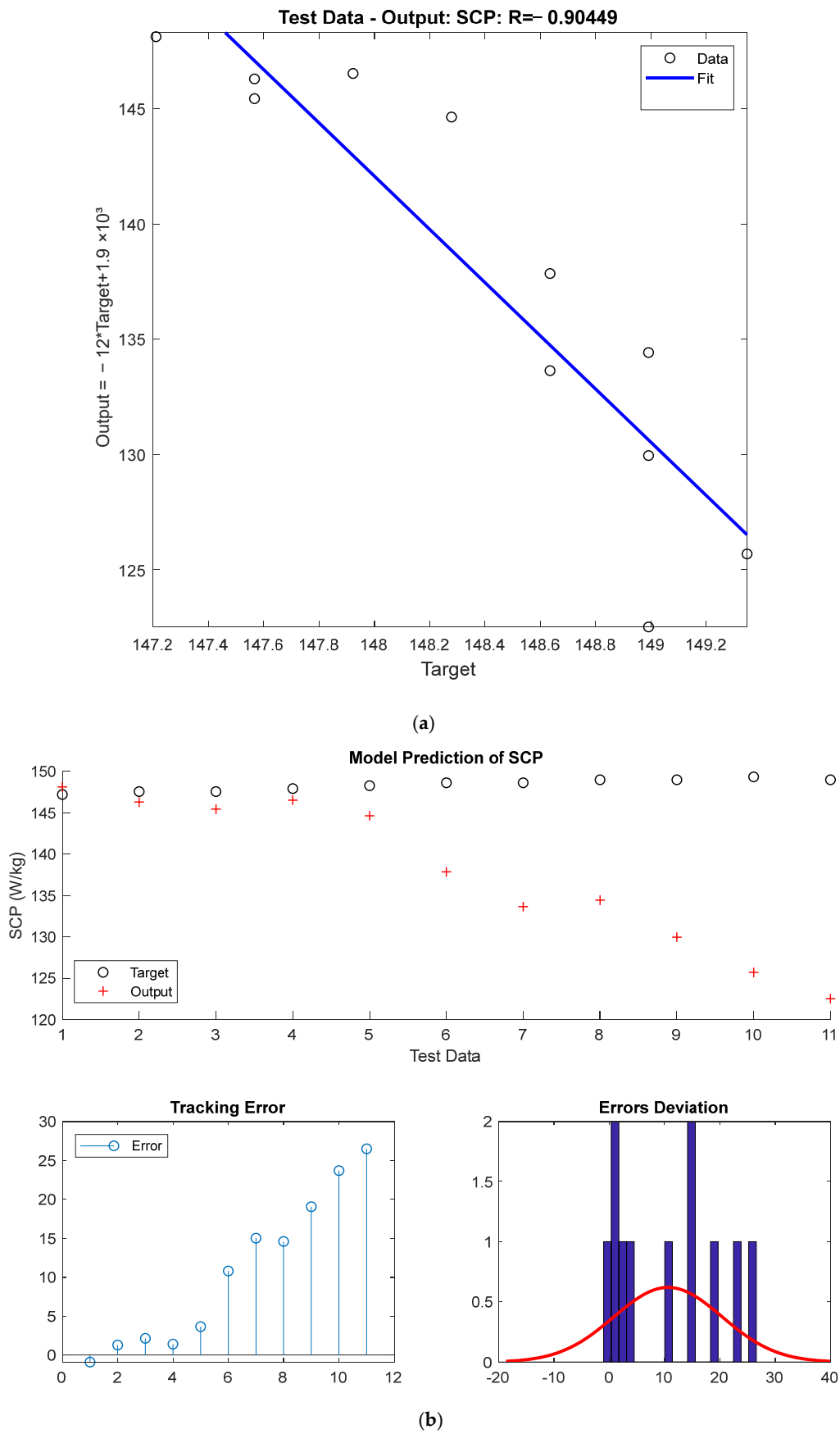


Figure 10. (a) Regression diagram of test data of RBF neural network for SCP parameter. (b) The test data error for the RBF model in predicting the SCP parameter.

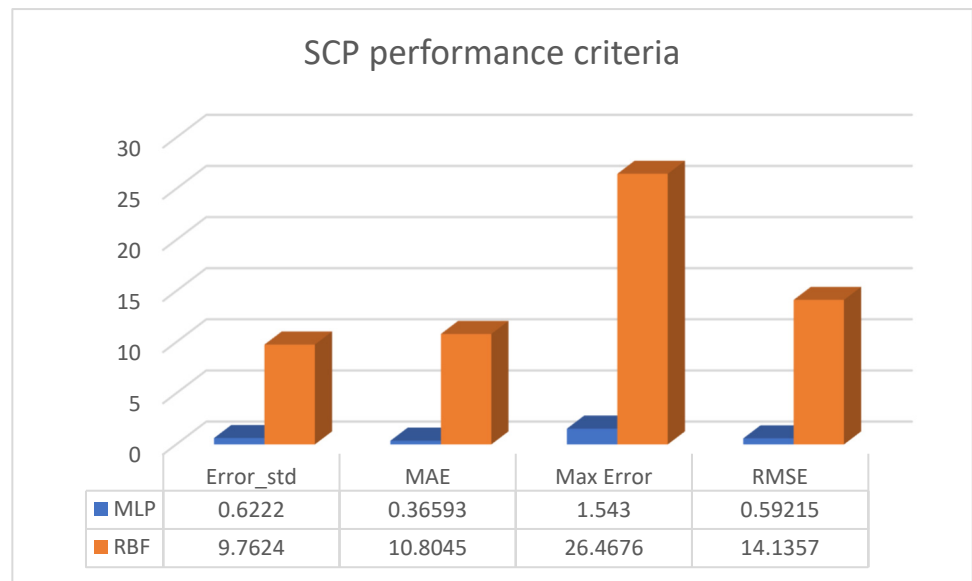


Figure 11. Evaluation metrics of MLP and RBF neural networks for SCP parameter.

6.1.3. Results of the Predicted Models for the SDWP Parameter

In order to evaluate the predicted models, the test data are used. Figures 12 and 13 present the output results for the SDWP output parameter obtained from the MLP and RBF neural network models, respectively:

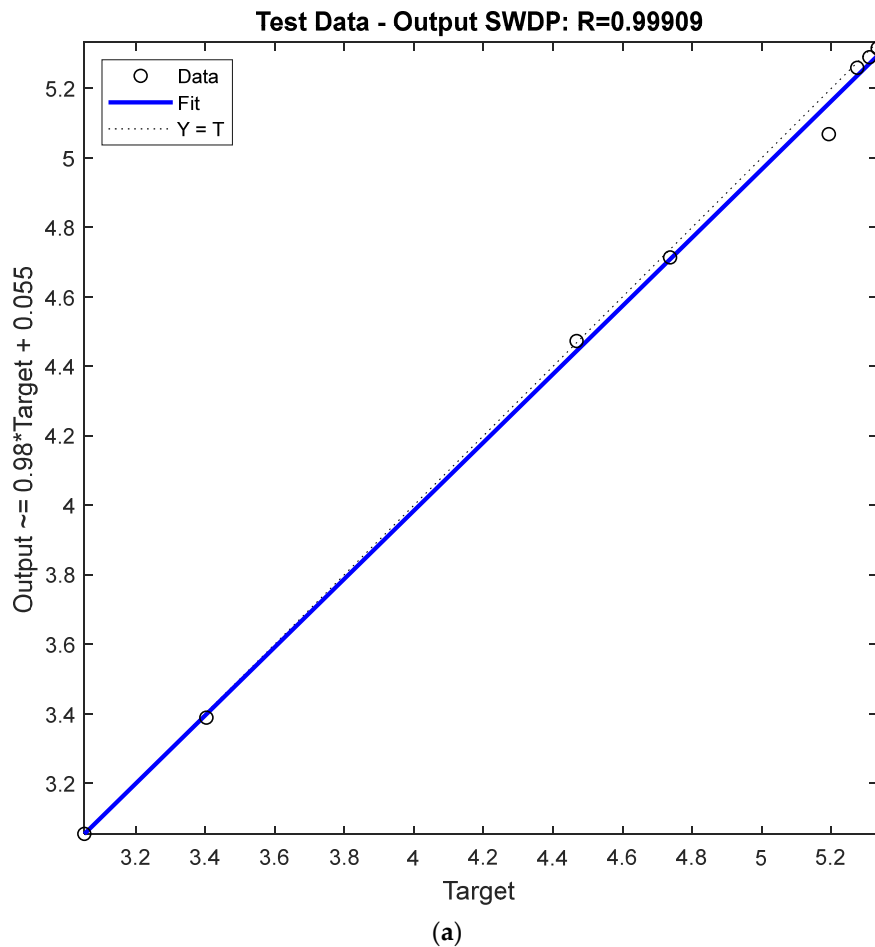


Figure 12. Cont.

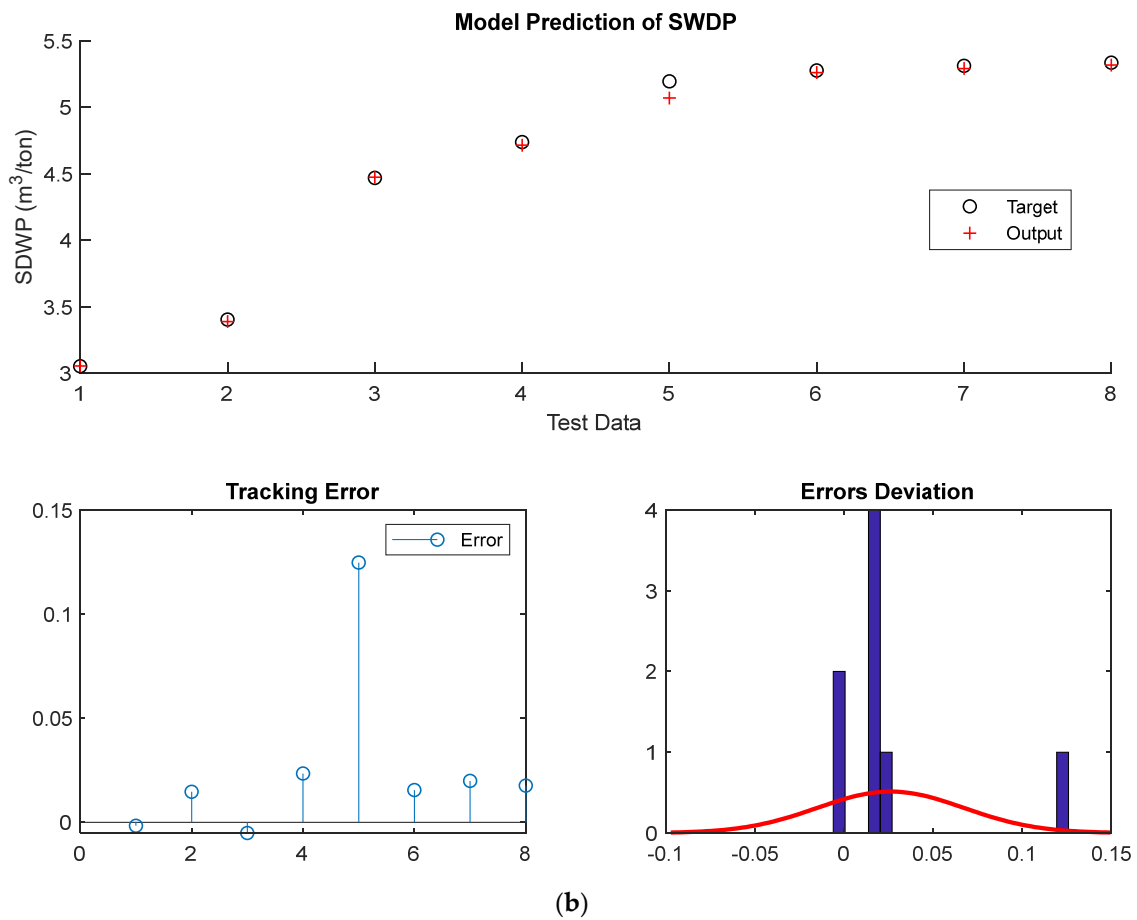


Figure 12. (a) Regression diagram of test data of MLP neural network for SWDP parameter. (b) The test data error for the MLP model in predicting the SWDP parameter.

Considering that a better model is designed whose regression (R) is closer to one and the value of its error indicators is closer to zero, from examining the regression diagram of both methods, it is concluded that the performance of the MLP is better and has a regression value of $R=0.999$ and RMSE value of 0.0465. Based on the analysis of error graphs and error histograms, it was observed that the radius-based functional neural network (RBF) had limited predictive capability for both the test and experimental data. Furthermore, by examining the RMSE indices, MAE, and other parameters in Figure 14, it was found that the MLP neural network had a better performance for predicting the SWDP parameter compared to the RBF neural network.

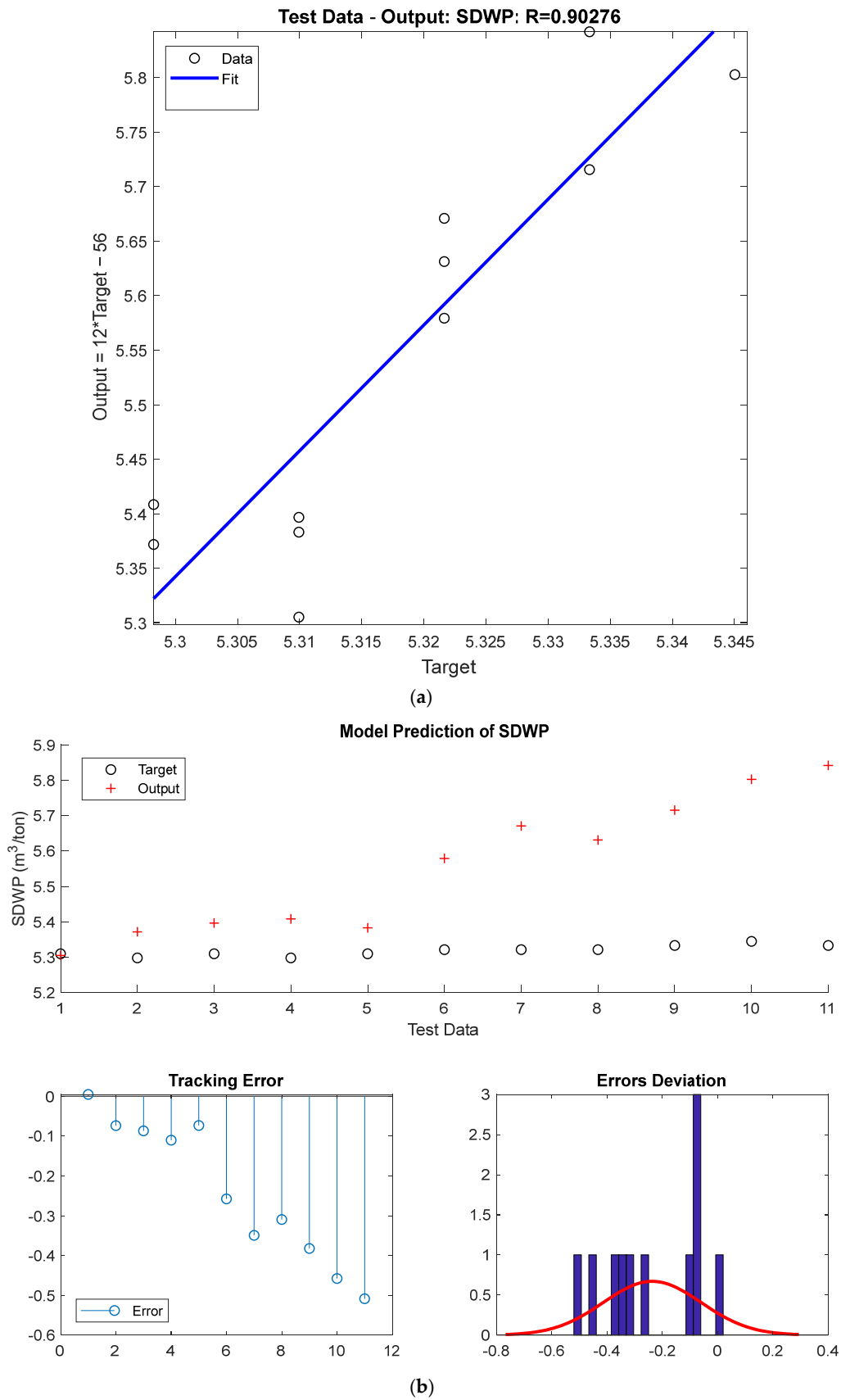


Figure 13. (a) Regression diagram of test data of RBF neural network for SWDP parameter. (b) The test data error for the RBF model in predicting the SWDP parameter.

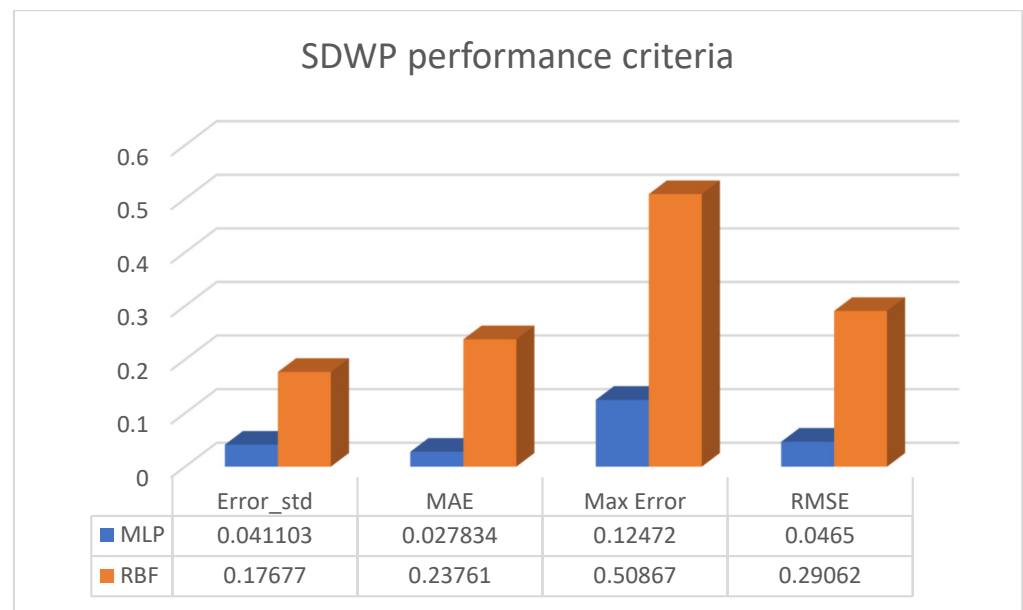


Figure 14. Evaluation metrics of MLP and RBF neural networks for SWDP parameter.

6.2. The Effect of Input Parameters on Network Output Parameters

6.2.1. The Result of Investigating the Impact of Input Variables for the COP Parameter

Based on the conducted investigations, it has been determined that there is a positive correlation between the inlet hot water temperature, the adsorption bed temperature, and the COP of the system. In other words, as these temperatures increase, the COP of the system also increases. Conversely, there is a negative correlation between the evaporator temperature and the COP of the system. This implies that as the evaporator temperature increases, the COP of the system falls. Eventually, the optimal temperature range for the evaporator is 18 °C, while the adsorption bed should be maintained at a temperature of 70 °C. The inlet hot water temperature is set at 75 °C, resulting in a system performance coefficient of 0.58. Based on the findings, it can be concluded that the impact of the inlet hot water temperature on the system is more significant than that of other parameters. By observing the aforementioned approach, one may discern the impact of the input parameters on the COP parameter presented below:

$$T_{HW} > T_{BED1} > T_{BED2} > T_{EVAP} > T_{COND} > 0.002$$

6.2.2. The Result of Investigating the Impact of Input Variables for the SCP Parameter

The findings of the investigations indicate that there is a positive correlation between the temperature of the adsorption bed, the temperature of the inlet hot water, and the SCP of the system. As these temperatures increase, the SCP also increases. Conversely, there is a negative correlation between the temperature of the system's evaporator and the rate of SCP. As the temperature of the evaporator increases, the rate of SCP decreases. So, the optimal temperature range for the inlet hot water is 75 °C, while the adsorption bed should also be maintained at 75 °C. On the other hand, the evaporator should be kept at a temperature of 18 °C.

Additionally, the cooling power rate of the system is measured at 149 W/kg of the absorber. Based on the findings, it can be concluded that the impact of the inlet hot water temperature on the system is more significant than that of other parameters. By observing the aforementioned approach, one may discern the impact of the input parameters on the SCP parameter presented below:

$$T_{HW} > T_{COND} > T_{BED2} > T_{BED1} > T_{EVAP} > 0.59215$$

6.2.3. The Result of Investigating the Impact of Input Variables for the SCWP Parameter

It can be concluded that the specific daily water production (SDWP) is positively related to both the temperature of the hot water coming in and the temperature of the evaporator by looking at the parameters that affect it. Conversely, the SDWP demonstrates a negative relationship between the temperature of the adsorption bed and the temperature of the condenser. Consequently, the optimal temperature range for the adsorption bed is 70 °C, while the condenser temperature should be maintained at 28 °C. Similarly, the evaporator temperature should be set at 26 °C, and the hot water inlet temperature should be maintained at 75 °C. Based on the findings, it can be concluded that the impact of the inlet hot water temperature on the system is more significant than that of other parameters. By observing the aforementioned approach, one may discern the impact of the input parameters on the SDWP parameter presented below:

$$T_{HW} > T_{EVAP} > T_{COND} > T_{BED1} > T_{BED2} > 0.0465$$

7. Conclusions

This study employs the multilayer perceptron neural network (MLP) and the radius-based functional neural network (RBF) to predict models for an adsorption desalination system. Through carrying out an examination of error diagrams and performing a comparative study of expected data from neural models, based on the empirical evidence, it is demonstrated that the MLP neural network outperforms the RBF neural network across all three output parameters, namely the coefficient of performance (COP), specific cooling power (SCP), and specific daily water production (SDWP). Considering the complexity of the adsorption desalination system, the effect of various parameters on the performance of the system in terms of water production and energy consumption was investigated. According to the investigation to ascertain the impact of the input parameters on the output parameters of the neural network, it was concluded that for all three functional parameters, COP, SCP, and SDWP, the parameter of hot water input to the system has the greatest impact on the output of the desalination system. The optimal temperature range for the evaporator is 18 °C, while the adsorption bed should be maintained at a temperature of 70 °C. The inlet hot water temperature is set at 75 °C, resulting in a system performance coefficient of 0.58.

Author Contributions: Conceptualization, T.Z. and M.C.; methodology, M.C. and T.Z.; software, M.C. and M.N.; validation, A.A., M.S.; formal analysis, T.Z. and A.A.; investigation, T.Z.; resources, T.Z. and M.N.; data curation, M.S.; writing—original draft preparation, M.N. and M.C.; writing—review and editing, T.Z. and M.C.; visualization, M.A.; supervision, T.Z. and M.S.; project administration, M.A.; funding acquisition, A.A. All authors have read and agreed to the published version of the manuscript.

Funding: This work was supported by the Iran National Science Foundation (4001793).

Data Availability Statement: Data is contained within the article.

Conflicts of Interest: The authors declare no conflict of interest.

References

1. Zarei, T.; Adibi, P. Operational analysis of a humidification–dehumidification desalination in packed bed humidifier and dehumidifier columns with salt- and freshwater recirculation. *J. Braz. Soc. Mech. Sci. Eng.* **2023**, *45*, 635. [[CrossRef](#)]
2. Zarei, T.; Miroliaei, M.R. Performance evaluation of an HDH desalination system using direct contact packed towers: Experimental and mathematical modeling study. *Water Reuse* **2022**, *12*, 92–110. [[CrossRef](#)]

3. Askalany, A.A.; Harby, K.; Ahmed, M.S. A state of the art of hybrid adsorption desalination–cooling systems. *Renew. Sustain. Energy Rev.* **2016**, *58*, 692–703. [[CrossRef](#)]
4. Askalany, A.A. Innovative mechanical vapor compression adsorption desalination (MVC-AD) system. *Appl. Therm. Eng.* **2016**, *106*, 286–292. [[CrossRef](#)]
5. Askalany, A.A.; Harby, K.; Ahmed, M.S. Performance evaluation of a solar-driven adsorption desalination-cooling system. *Energy* **2017**, *128*, 196–207. [[CrossRef](#)]
6. Amirfakhraei, A.; Zarei, T.; Khorshidi, J. Theoretical analysis of an improved adsorption desalination system under different operating conditions. *Proc. Inst. Mech. Eng. Part E J. Process. Mech. Eng.* **2021**, *235*, 768–778. [[CrossRef](#)]
7. Amirfakhraei, A.; Khorshidi, J.; Zarei, T. A thermodynamic modeling of 2-bed adsorption desalination to promote main equipment performance. *J. Water Reuse Desalinat.* **2021**, *11*, 136–146. [[CrossRef](#)]
8. Bakhshandeh, M.H.; Zarei, T.; Khorshidi, J.J.C.P.D. CFD study on Beds of an Adsorption desalination system in order to improve bed performance. *J. Chem. Process Des.* **2022**, *1*, 60–74.
9. Zejli, D.; Benchrif, R.; Bennouna, A.; Bouhelal, O.K. A solar adsorption desalination device: First simulation results. *Desalination* **2004**, *168*, 127–135. [[CrossRef](#)]
10. Wang, X.; Chakraborty, A.; Ng, K.C.; Saha, B.B. How Heat and Mass Recovery Strategies Impact the Performance of Adsorption Desalination Plant: Theory and Experiments. *Heat Transf. Eng.* **2007**, *28*, 147–153. [[CrossRef](#)]
11. Mitra, S.; Kumar, P.; Srinivasan, K.; Dutta, P. Instrumentation and control of a two-stage 4-bed silica gel+water adsorption cooling cum desalination system. *Measurement* **2016**, *79*, 29–43. [[CrossRef](#)]
12. Ali, S.M.; Chakraborty, A. Adsorption assisted double stage cooling and desalination employing silica gel + water and AQSOA-Z02 + water systems. *Energy Convers. Manag.* **2016**, *117*, 193–205. [[CrossRef](#)]
13. Amirfakhraei, A.; Zarei, T.; Khorshidi, J. Performance Improvement of Adsorption Desalination System by Applying Mass and Heat Recovery Processes. *Therm. Sci. Eng. Prog.* **2020**, *18*, 100516. [[CrossRef](#)]
14. Zarei, T.; Behyad, R. Predicting the water production of a solar seawater greenhouse desalination unit using multi-layer perceptron model. *Sol. Energy* **2019**, *177*, 595–603. [[CrossRef](#)]
15. Zarei, T.; Behyad, R.; Abedini, E.J.D. Study on parameters effective on the performance of a humidification-dehumidification seawater greenhouse using support vector regression. *J. Desalinat.* **2018**, *435*, 235–245. [[CrossRef](#)]
16. Essa, F.; Elaziz, M.A.; Elsheikh, A.H. An enhanced productivity prediction model of active solar still using artificial neural network and Harris Hawks optimizer. *Appl. Therm. Eng.* **2020**, *170*, 115020. [[CrossRef](#)]
17. Cabrera, P.; Carta, J.A.; González, J.; Melián, G. Wind-driven SWRO desalination prototype with and without batteries: A performance simulation using machine learning models. *Desalination* **2018**, *435*, 77–96. [[CrossRef](#)]
18. Jafari, S.; Hoseinzadeh, S.; Sohani, A. Deep Q-Value Neural Network (DQN) Reinforcement Learning for the Techno-Economic Optimization of a Solar-Driven Nanofluid-Assisted Desalination Technology. *Water* **2022**, *14*, 2254. [[CrossRef](#)]
19. Abba, S.I.; Usman, J.; Abdulazeez, I.; Lawal, D.U.; Baig, N.; Usman, A.G.; Aljundi, I.H. Integrated Modeling of Hybrid Nanofiltration/Reverse Osmosis Desalination Plant Using Deep Learning-Based Crow Search Optimization Algorithm. *Water* **2023**, *15*, 3515. [[CrossRef](#)]
20. Ma, X.; Lan, C.; Lin, H.; Peng, Y.; Li, T.; Wang, J.; Azamat, J.; Liang, L. Designing desalination MXene membranes by machine learning and global optimization algorithm. *J. Membr. Sci.* **2024**, *702*, 122803. [[CrossRef](#)]
21. Faegh, M.; Behnam, P.; Shafii, M.B.; Khiadani, M. Development of artificial neural networks for performance prediction of a heat pump assisted humidification-dehumidification desalination system. *Desalination* **2021**, *508*, 115052. [[CrossRef](#)]
22. Shahouni, R.; Abbasi, M.; Dibaj, M.; Akrami, M. Utilising Artificial Intelligence to Predict Membrane Behaviour in Water Purification and Desalination. *Water* **2024**, *16*, 2940. [[CrossRef](#)]
23. Alhumade, H.; Rezk, H.; Al-Zahrani, A.A.; Zaman, S.F.; Askalany, A. Artificial Intelligence Based Modelling of Adsorption Water Desalination System. *Mathematics* **2021**, *9*, 1674. [[CrossRef](#)]
24. Zayed, M.E.; Ghazy, M.; Shboul, B.; Elkadeem, M.R.; Rehman, S.; Irshad, K.; Abido, M.A.; Menesy, A.S.; Askalany, A.A. Enhanced performance of a hybrid adsorption desalination system integrated with solar PV/T collectors: Experimental investigation and machine learning modeling coupled with manta ray foraging algorithm. *Appl. Therm. Eng.* **2024**, *255*, 124023. [[CrossRef](#)]
25. Ullah, I.; Rasul, M.G. Recent Developments in Solar Thermal Desalination Technologies: A Review. *Energies* **2018**, *12*, 119. [[CrossRef](#)]
26. Du, B.; Gao, J.; Zeng, L.; Su, X.; Zhang, X.; Yu, S.; Ma, H. Area optimization of solar collectors for adsorption desalination. *Sol. Energy* **2017**, *157*, 298–308. [[CrossRef](#)]
27. Wu, J.W.; Hu, E.J.; Biggs, M.J. Thermodynamic cycles of adsorption desalination system. *Appl. Energy* **2012**, *90*, 316–322. [[CrossRef](#)]
28. Amirfakhraei, A.; Zarei, T.; Khorshidi, J. Advanced heat and mass recovery design in a two bed adsorption desalination system. *Appl. Therm. Eng.* **2021**, *198*, 117494. [[CrossRef](#)]
29. Chan, K.Y.; Abu-Salih, B.; Qaddoura, R.; Al-Zoubi, A.M.; Palade, V.; Pham, D.-S.; Del Ser, J.; Muhammad, K. Deep neural networks in the cloud: Review, applications, challenges and research directions. *Neurocomputing* **2023**, *545*, 126327. [[CrossRef](#)]
30. Liu, J. *Radial Basis Function (RBF) Neural Network Control for Mechanical Systems: Design, Analysis and Matlab Simulation*; Springer Science & Business Media: Berlin/Heidelberg, Germany, 2013.

-
31. Engelbrecht, A.P. *Computational Intelligence: An Introduction*; John Wiley & Sons: Hoboken, NJ, USA, 2007.
 32. Haykin, S. *Neural Networks and Learning Machines*, 3rd ed.; Pearson Education: London, UK, 2009.

Disclaimer/Publisher's Note: The statements, opinions and data contained in all publications are solely those of the individual author(s) and contributor(s) and not of MDPI and/or the editor(s). MDPI and/or the editor(s) disclaim responsibility for any injury to people or property resulting from any ideas, methods, instructions or products referred to in the content.